Available online at www.sciencedirect.com
ScienceDirect
Bioorganic & Medicinal Chemistry 16 (2008) 354–361
Bioorganic & Medicinal Chemistry

Amide bond direction modulates G-quadruplex recognition and telomerase inhibition by 2,6 and 2,7 bis-substituted anthracenedione derivatives

Giuseppe Zagotto,[a] Claudia Sissi,[a] Stefano Moro,[a] Diego Dal Ben,[d] Gary N. Parkinson,[c] Keith R. Fox,[b] Stephen Neidle[c] and Manlio Palumbo[a,*]

[a]*Department of Pharmaceutical Sciences, University of Padova, Via Marzolo, 5, 35131 Padova, Italy*
[b]*School of Biological Sciences, University of Southampton, Bassett Crescent East, Southampton SO16 7PX, UK*
[c]*CRUK Biomolecular Structure Group, The School of Pharmacy, University of London, London WC1N 1AX, UK*
[d]*Department of Chemical Sciences, University of Camerino, Via S.Agostino, 1, 62032 Camerino(MC), Italy*

Received 2 July 2007; revised 11 September 2007; accepted 19 September 2007
Available online 25 September 2007

Abstract—G-quadruplex structures of DNA represent a potentially useful target for anticancer drugs. Stabilisation of this arrangement at the ends of chromosomes may inhibit the action of telomerase, an enzyme involved in immortalization of cancer cells. Appropriately substituted amido anthracenediones are effective G-quadruplex stabilizers, but no information is available as yet on the possible modulation of G-quadruplex recognition and telomerase inhibition produced by the direction of the amide bond. To understand the basis of amido anthracenedione selectivity, we have synthesized a number of derivatives bearing the –CO–NH– or –NH–CO– group linked to the planar anthraquinone (AQ) moiety at 2,6 and 2,7 positions. The various isomers were tested in terms of telomerase inhibition, determined by the TRAP assay, G-quadruplex stabilisation measured by the increase in melting temperature of the appropriately folded oligonucleotide using FRET, and conformational and G4 binding properties examined by molecular modelling techniques. In all cases, enzymatic inhibition and G-quadruplex stabilization were directly related, which strongly supports the proposed molecular mechanism of telomerase interference. Interestingly, the AQ–NH–CO– arrangement performs invariantly better than the AQ–CO–NH– arrangement, showing a clear preference among isomeric derivatives. Theoretical calculations suggest that the former amide arrangement is co-planar with the aromatic system, whereas the latter is tilted by about 30° when considering the most stable conformation. A more extended planar surface would allow more efficient stacking interactions with the quadruplex structure, hence more effective telomerase inhibition.

1. Introduction

Telomeres are DNA sequences located at the terminal ends of all chromosomes.[1] They consist of tandem repeats of guanine rich sequences (5′-TTAGGG in humans) which cap the ends of chromosomes, protecting them from deleterious processes such as fusion, recombination or loss of genetic information during replication steps. Indeed, due to the so called 'end-replication problem' telomeres shorten after each doubling in normal cells. When the number of tandem repeats falls below a critical value (Hayflick number), the cell enters senescence and eventually, if it can undergo additional cell division cycles, into apoptosis.[2] Undifferentiated cells, however, have the facility to maintain telomere length constant as they express a nucleoprotein, telomerase, consisting of an RNA subunit that provides the nucleic acid template and a protein catalytic subunit, which is able to add telomeric sequences at the 3′ terminal of chromosomes.[3]

The interest in telomerase as an anticancer drug target stems from the observation that telomerase is activated in ca 85% of human cancers, but it is silent, or expressed at very low levels in normal somatic cells.[4] Telomerase prevents cells from entering senescence and ensures that they remain immortal. Hence, inhibiting this enzyme would allow telomere shortening and finally cell death to occur. At present, among different strategies actively pursued to inhibit telomerase activity in cancer cells, the development of G-quadruplex stabilizers has emerged as a highly promising approach.[5] This is based on the fact

Keywords: Anthracenedione; G-quadruplex; Telomerase; Cancer.
* Corresponding author. Tel.: +39 049 8275699; fax +39 049 8275366; e-mail: manlio.palumbo@unipd.it

0968-0896/$ - see front matter © 2007 Elsevier Ltd. All rights reserved.
doi:10.1016/j.bmc.2007.09.040

that single-stranded G-rich telomeric repeats, in the presence of monovalent cations, are able to assemble into quadruplex DNA structures stabilized by guanine tetrads. Since telomerase reverse transcriptase activity depends on the 3′ single-stranded telomeric DNA end acting as a primer, small molecules that bind and stabilize the folded quadruplex form of the primer can inhibit enzyme action. Efficient inhibitors are generally characterized by the presence of an extended planar system which stacks on the guanine tetrad, together with two or three positively-charged side-chains located in the DNA grooves, which additionally stabilize the resulting complex through charge interactions. To date, a number of families of compounds have been identified and their interactions with G-quadruplexes have been extensively studied.[6] The cellular effects produced by several such compounds have now been studied in detail, and indicate that classic telomerase inhibition does occur, with subsequent telomere length attrition. However more rapid senescence and apoptosis effects occur, which have been ascribed to quadruplex formation promoting dissociation of single-strand binding proteins such as hPOT1 and uncapping of telomerase from the 3′ end of the telomere.[7] Exposure of the 3′ end as a quadruplex-ligand complex then acts as a DNA damage response signal. Among the quadruplex ligands studied, disubstituted amido-anthraquinones represent an example of how the pattern of disubstitution modulates DNA duplex vs. quadruplex selectivity. In fact, the presence of 1,4 substituents shifts the binding preference to the duplex structure, whereas 2,6 or 2,7 congeners prefer G-quadruplex arrangements.[8]

One of the issues remaining still unexplored is an assessment of the role, if any, played by the amide bond direction in amido-anthraquinones, that would favour G-quadruplex recognition. In this connection, we prepared and examined anthraquinone derivatives (AQ) characterised by two identical side chains at positions 2 and 6 or 2 and 7, linked to the aromatic ring by an amide bond as reported in Figure 1. The choice of the side chain groups rests on the effective anti-telomerase activity they exhibited in previous studies.[8] The AQ–CO–NH– group was labelled as the amide-form and the AQ–NH–CO– as the '*inverse*' amide-form.

2. Synthetic procedures

Reaction of 1,4-benzoquinone with 2 equivalents of isoprene at 130 °C under pressure gave the mixed 2,6 and 2,7- Diels-Alder adducts in 48% yield. The 2,6 and 2,7 isomers could be separated after oxidation of the above adducts with oxygen to the anthraquinones. In fact, the 2,6-isomer is completely insoluble in ethanol and can be filtered off.

Both 2,6 and 2,7-dimethylanthraquinones can be oxidized to the di-acid in 77% yield by refluxing in glacial acetic acid with chromium trioxide.

The acid chlorides of the 2,6 and 2,7-diacid anthraquinones were obtained using thionyl chloride in THF and these were converted, in the same pot, to the 2,6 and 2,7-Boc-ethylenediamido- anthraquinones using mono-protected Boc-ethylenediamine in THF. The Boc protecting group was finally removed using 90% Trifluoroacetic acid (TFA) in water. The synthesis of anthracenedione-peptide **2,6-AQ–CO–NH** conjugates (ethylenediamide anthraquinones or ED-AQ) is shown in Scheme1. The same procedure was applied to obtain the **2,7-AQ–CO–NH** derivatives (numbered with a prime: 1′, 2′, 3′, etc.).

The 2,6-diaminoanthraquinone is commercially available, however the 2,7-diaminoanthraquinone is not. According to previously reported protocols, the 2,7-diaminoanthraquinone was obtained by Zinin reduction of 2,7-dinitroanthraquinone using sodium sulfide nonohydrate, prepared, in turn, by the oxidative nitration of anthrone[8d] (see Scheme 1).

The acid chloride of Fmoc-βAla-OH was generated by reaction of the acid with thionyl chloride. The Fmoc-βAla-Cl was then coupled with the 2,6- or 2,7-diaminoanthraquinone in refluxing THF for 7 h to give the

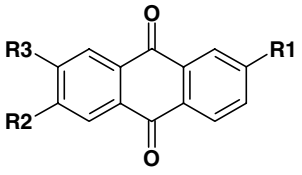

Compound	*R1*	*R2*	*R3*
4	-CO-NH-$(CH_2)_2$-NH_3^+	-CO-NH-$(CH_2)_2$-NH_3^+	H
4'	-CO-NH-$(CH_2)_2$-NH_3^+	H	-CO-NH-$(CH_2)_2$-NH_3^+
5	-CO-NH-$(CH_2)_2$-pyrrolidine	-CO-NH-$(CH_2)_2$-pyrrolidine	H
5'	-NH-CO -$(CH_2)_2$-pyrrolidine	-NH-CO-$(CH_2)_2$-pyrrolidine	H
10	-NH-CO-$(CH_2)_2$-NH_3^+	-NH-CO-$(CH_2)_2$-NH_3^+	H
10'	-NH-CO-$(CH_2)_2$-NH_3^+	H	-NH-CO-$(CH_2)_2$-NH_3^+

Figure 1. Chemical structures of tested compounds.

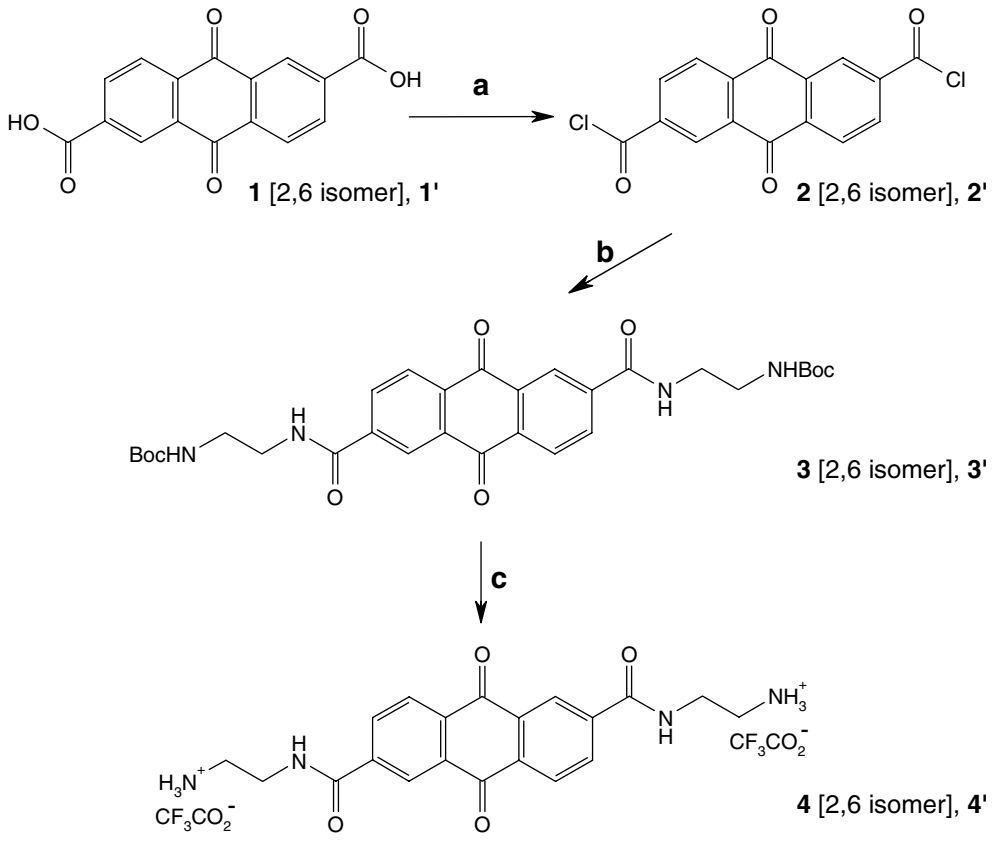

Scheme 1. Reagents and conditions. (a) $SOCl_2$, THF, reflux, 6 h; (b) Boc-ethylenediamine, NEt_3, THF, reflux, 3 h; (c) TFA, water, rt, 1 h.

2,6-Fmoc-ethylenediamine reverse amide anthraquinones as shown in Scheme 2. The 2,6-bis-[*N*-(3-Fmoc-amino)-propionamide] anthraquinones were then deprotected in DMF and the free amines were treated with 90% trifluoroacetic acid (TFA) in water to give the 2,6-bis-(3-amino)-propionamide anthraquinones. Also, active ester couplings between the 2,6-diaminoanthraquinone and Fmoc-βAla-OH using EDCI/HOBt and HBTU/HOBt did not work either and only starting material could be recovered. This is due to the

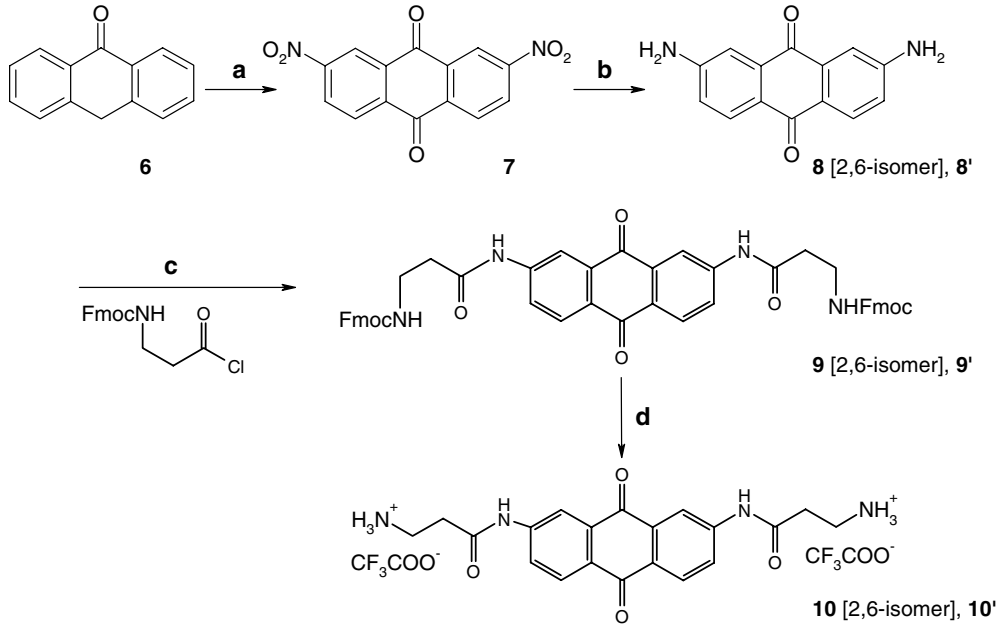

Scheme 2. Reagents and conditions. (a) HNO_3, 0–5°C, 2 h—AcOH, reflux, 2 h; (b) $Na_2S.9H_2O$, NaOH, EtOH, reflux, 6 h; (c) Fmoc-b-Ala-Cl, THF, 7 h; (d) piperidine, DMF, rt 2 h—TFA/water.

low solubility of the 2,6-diaminoanthraquinone. The synthesis of anthracenedione-peptide **2,6-AQ–NH–CO** conjugates (2,6-Fmoc-β-Ala-AQ) and of the **2,7-AQ–NH–CO** derivatives (numbered with a prime: 1′, 2′, 3′, etc.) is shown in Scheme 2.

2,6-Bis[3-(1-pyrrolidino)]propionamido]anthracene-9,l0-dione **5** was prepared as described[8e] but reacting 2-bromopropionylbromide with the 2,6-diaminoanthracene-9,10-dione while the analogous 2,6-bis-[3-(1-pyrrolidino)propionamido]anthracene-9,10-dione **5′** was obtained reacting the cloride **2** and 2-bromoethylammine and then substititing the bromine in the 2,6-bis-(3-bromopropionamido)anthracene-9,10-dione with pyrrolidine.

3. Telomerase inhibition

All purified anthraquinones were assayed for telomerase inhibition by a modified telomere repeat amplification protocol (TRAP) assay,[9] using a JR8 cell extract. At the drug concentrations used, no TAQ-mediated DNA amplification was observed.[10]

Results are summarized in Table 1.

All test derivatives showed telomerase inhibition activity in the micromolar range, although with variable efficiency.

When comparing the differences in potency between derivatives carrying the two different amide linkages, it clearly emerged that compounds presenting the inverse amide link are consistently more efficient in interfering with the enzymatic activity.

The activity ratio is close to 4 for 2,6 derivatives but increases up to 12 for 2,7 derivatives.

4. G-quadruplex stabilisation

To confirm that telomerase inhibition rests on G-quadruplex recognition, ligand interaction with telomeric G-quadruplexes was investigated using a synthetic oligonucleotide formed by four repeats of the human telomeric sequence, $(GGGTTA)_4$, containing a fluorophore (fluorescein) at the 5′-end and a quencher (MethylRed) at the 3′-end.[11] When this sequence folds into an intramolecular G-quadruplex, fluorescein and MethylRed are in close proximity and the fluorescence is quenched, whereas, when DNA denaturation occurs, they move apart and a large increase in the fluorescence signal is observed. The mid point of this temperature transition (T_m) is related to G-quadruplex stability. Ligands that bind effectively to this structure produce an increase in the melting temperature, which provides a reliable indication of the G-quadruplex affinity for different compounds.

The results obtained using the test AQs at two concentrations in 50 mM potassium phosphate buffer, pH 7.4, are reported in Table 1. A representative example is shown in Figure 2.

All derivatives stabilise the G-quadruplex structure, which is indicative of effective binding. Interestingly, derivatives characterised by the '*inverse*' amide form are more efficient stabilisers as they extensively increase thermal stability at drug concentration as low as 1 μM, which is close to the IC_{50} values for telomerase inhibition. Further increase in AQ concentration induced a more pronounced shift in the oligonucleotide melting temperature. These experimental data further confirm that amido-anthraquinones containing the AQ–NHCO– linkage binds more efficiently to G-quadruplex structures than those containing the AQ–CO–NH– linkage.

Melting experiments were also performed with $(GGGTTA)_4$ annealed to its complementary sequence to start form a double helical arrangement. In these experiments two transitions were observed, one corresponding to the change from duplex to quadruplex, the other referring to quadruplex melting. Hence, differential stabilization of G-quadruplex vs. double helix by

Table 1. Telomerase inhibition EC_{50} and thermal stabilization of human telomeric G-quadruplex by test amido-anthraquinones

Compound	EC_{50} (μM)	Ratio[a]	ΔT_m (°C)	
			1 μM	10 μM
4	5.2 ± 0.4	4.3	2.0 ± 0.2	10.0 ± 0.3
10	1.2 ± 0.3		9.1 ± 0.3	18.1 ± 0.3
5	10.4 ± 0.4	4.2	1.8 ± 0.3	10.8 ± 0.3
5′	2.5 ± 0.4		5.9 ± 0.3	19.2 ± 0.3
4′	14.5 ± 0.4	12.1	3.3 ± 0.2	12.9 ± 0.3
10′	1.2 ± 0.3		11.3 ± 0.3	27.3 ± 0.3

[a] Ratio of the IC_{50} values obtained for the compound containing the linker in the amide form and in the '*inverse*' amide form, respectively.

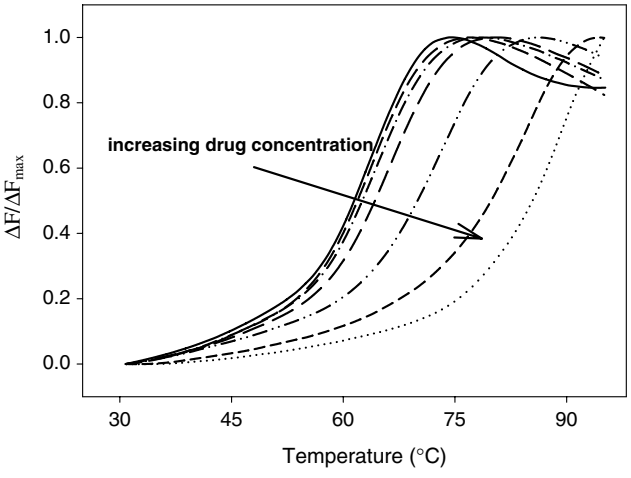

Figure 2. Fluorescence melting curves of end-labelled $(GGGTTA)_4$ recorded in the absence (solid line) and in the presence of increasing concentrations of compound **10′** (dashed lines) in 50 mM potassium phosphate buffer, pH 7.4. Ligand concentrations were 0.5; 1.0; 2.0; 5.0 and 10.0 μM., respectively. Curves are normalized in terms of relative fluorescence changes.

the test drugs could be monitored. Indeed, the first transition was poorly affected by drug presence (ΔT_m max 4 °C at 10 μM) and essentially independent upon the nature of the side-chains. On the contrary, the second transition was effectively stabilised by the test anthracenediones, the inverse amide form producing remarkably higher quadruplex stabilisation. While confirming the results previously described, these data show modest double helix stabilisation by the test drugs and clear-cut preference for the G-quadruplex arrangement.

5. Conformational and modelling studies

To explain the molecular basis for preferential recognition of G-quadruplexes by amido-anthraquinones having the '*inverse*' amide bond, a systematic conformational analysis was performed to describe and compare the conformational space generated by the rotation of both AQ–NH–CO– and AQ–CO–NH– dihedrals.

As shown in Figure 3, the inverse amide is characterized by a deep potential energy minimum corresponding to a perfect co-planar arrangement ($\phi = 0°$) of the AQ–NH–CO– (*inverse* amide) dihedral. On the contrary, the AQ–CO–NH– dihedral reaches its energy minimum in correspondence of a torsional angle of 30°. Hence, in this case a tilt conformation seems to represent the most stable arrangement. It is noteworthy the non-symmetrical shape of the curve in the left panel, which is consistent with loss of planarity of the amide nitrogen substituents. Considering that the likely molecular mechanism of action of these AQ-based telomerase inhibitors rests upon G-quadruplex stabilisation, it can be inferred that the derivative showing the largest planar surface can better recognize, mainly through π–π interactions, the quadruplex target structure. Qualitative molecular modelling (Fig. 4) using a two-quadruplex model for human telomeric DNA indicates that the reverse amide substitution results in improved interactions compared to the normal amide molecules; more detailed computations of interaction energies will be undertaken in the future.

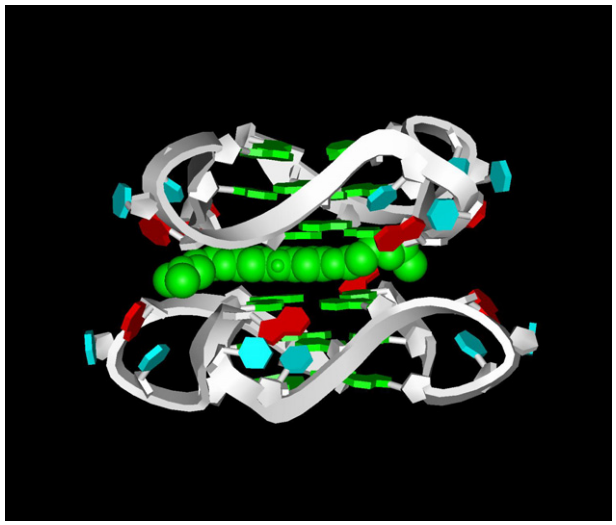

Figure 4. Molecular model of compound **10** bound in a low-energy position to a 45-nucleotide human quadruplex dimer molecule constructed from two of the units determined crystallographically.[15]

In conclusion, the data presented here show that the direction of the amide bond connecting the side chains to the anthraquinone moiety plays a critical role in modulating telomerase inhibition. According to the proposed mode of action of this class of compounds, the observed differences are linked to the extension of the drug's planar surface which confirms the importance of stacking interactions onto the G-quartet arrangement for effective telomerase inhibition. A large planar structure of the G-quadruplex binder plays an additional role in enhancing selectivity. In fact, besides

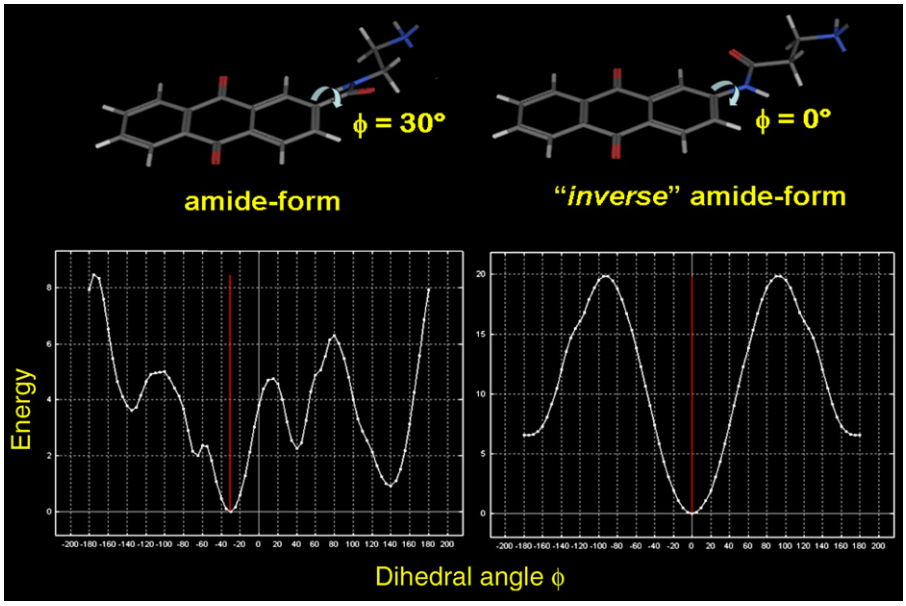

Figure 3. Conformational analysis of both amide- and '*inverse*' amide form of the newly synthesized anthracenedione derivatives.

increasing the energy of interaction with the nucleic acid target arranged as a G-quaduplex, it renders intercalation into a double helix less likely. Accordingly, future design of G-quadruplex-directed amidoanthraquinone derivatives for effective telomerase inhibition should preferentially consider the '*inverse*' direction of the amide bond.

6. Experimental

Chemicals, reagents and solvents, were purchased from Aldrich or Fluka and used without further purification. Aminoacids were from Novabiochem. ^{1}H and ^{13}C NMR spectra were recorded on a Bruker AMX300 spectrometer in deuterated methyl sulfoxide (DMSO-d_6) from Cambridge Lab. and referenced to TMS (δ scale). Chromatography and flash chromatography were performed using silica gel Merck 60 (70-230 mesh) and Merck 60 (0.040-0.063 mm), respectively. TLC plates were also from Merck: Merck 60 F-254, 0.25 mm precoated plates. Melting points were determined in capillary tubes and are uncorrected using a Gallenkamp apparatus. Elemental analysis (C, H, N) were performed by the Microanalytical Laboratory of the Department of Pharmaceutical Sciences of the University of Padova on a within 0.40% of the calculated values and were performed on a Carlo Erba 1016 Elemental Analyser. Exact masses (HRMS) were obtained from a Electrospray mass spectra were obtained using a Mariner™ API-TOF (Perseptive Biosystems Inc.- Framingham MA 01701, USA).

Within the experimental part AQ stays for anthraquinone, ED for 1,2-ethylenediamine and β-Ala for β-Alanine.

Both the 2,6 and 2,7-dimethylanthracene-9,10-diones were obtained using a previously-reported procedure.[12]

6.1. 2,6-Dicarboxyanthracene-9,10-dione (1)

2,6-Dimethyanthracene-9,10-dione (4.04 g, 17.10 mmol) was dissolved in glacial acetic acid (220 mL) and CrO_3 (26.44 g, 264.00 mmol) was added. The mixture was heated to reflux for 24 h (the colour changed form orange to green). The cooled mixture formed a precipitate that was collected, washed several times with water until the supernatant was colourless, and then with acetone. Product **1** was obtained as slightly yellow powder (3.92 g, yield 77%).

^{1}H NMR (DMSO-d_6): δ 13.77 (bs, 2H), 8.81 (s, 2H), 8.48 (d, J = 7.9 Hz, 2H), 8.40 (d, J = 7.9 Hz, 2H); ^{13}C NMR (DMSO-d_6): δ 182.47, 166.50, 139.45, 137.03, 136.47, 135.44, 134.14, 128.33.

6.2. 2,7-Dicarboxyanthracene-9,10-dione (1′)

2,7-Dimethyanthracene-9,10-dione (4.04 g, 17.10 mmol) was oxidized as decribed before for the 2,6-isomer. Product **1′** was obtained as slightly yellow powder (3.88 g, yield 76%).

^{1}H NMR (DMSO-d_6): δ 13.75 (bs, 2H), 8.78 (s, 2H), 8.46 (d, J = 7.9 Hz, 2H), 8.37 (d, J = 7.9 Hz, 2H); ^{13}C NMR (b, DMSO-d_6): δ 182.47, 182.17, 166.70, 136.64, 136.38, 135.42, 133.98, 134.14, 128.32.

6.3. 2,6-and 2,7-dicarboxyl-anthraquinones chloride (2 and 2′)

2,6- (or 2,7-dicarboxyl-anthraquinone) **1** or **1′** (0.70 g, 2.38 mmol) was suspended in dry THF (150 mL). To the suspension was added freshly distilled thionyl chloride (1.73 mL, 23.81 mmol) and the reaction mixture refluxed for 7 h. The solvent was removed in vacuo and the product was washed with chloroform (3 × 60 mL) to remove any residual thionyl chloride. The 2,6- and 2,7- dicarboxyl-anthraquinone chloride **2** and **2′** were used without any further purification or characterization directly in the next reaction (quantitative yield assumed).

6.4. 2,6- and 2,7-Boc protected ethylenediamide anthraquinones (3 and 3′)

In a 250 mL round bottomed flask flushed with nitrogen were introduced the 2,6- (or 2,7-dicarboxyl-anthraquinone chloride) (5.07 mmol) and dry tetrahydrofuran (150 mL). To the stirring solution was added triehylamine (11.1 mol) and then the *N*-(*tert*-butoxycarbonyl)ethylenediamine (9.9 mmol) in dry tetrahydrofuran (5 mL) and the reaction mixture was warmed to reflux for 3 h. The reaction mixture was allowed to cool down to 0 °C and left for 1 h. The resulting suspension was transferred in to two 50 mL centrifuge tubes and spun at 4500 rpm for 5 min at +4 °C.

The supernatant was removed and the solid washed with water (5 × 20 mL). The solid product was dried in vacuo for 4 h at 50 °C to give the 2,6-Boc protected ethylenediamideanthracene-9,10-dione (3.9 mmol, 68%) or 2,7-Boc protected ethylenediamideanthracene-9,10-dione (2.66 mmol, 52%).

^{1}H NMR (DMSO-d_6): δ 8.95 (bs,2H), 8.66 (s, 2H), 8.32 (d, J = 7.7 Hz, 2H), 8.29 (d, J = 7.7 Hz, 2H), 6.95 (bs, 2H), 3.33 (m, 4H), 3.16 (m, 4H), 1.37 (s, 18H).

6.5. 2,6- and 2,7- ethylenediamide anthraquinones TFA salt (4 and 4′)

In a 250 mL round bottomed flask were introduced the 2,6- (or 2,7-) Boc protected ethylenediamideanthracene-9,10-dione (2.0 mmol) and 90% trifluoroacetic acid water (50 mL). The reaction mixture was stirred 1 h at room temperature and then cooled to 0 °C. To the reaction mixture was added cold diethyl ether (120 mL) and resulting solid was transferred in to two 50 mL centrifuge tubes. The solid was spun at 4500 rpm for 5 min at +4 °C. The supernatant was removed and discarded and the solid product in each of the centrifuge tubes was washed with diethyl ether (5 × 30 mL) to remove any excess trifluoroacetic acid. The solid product was dried in vacuo for 1 h to give 2,6-ethylenediamideanthracene-9,10-dione TFA salt as a pale yellow solid

(0.002 mol, 100%) or the 2,7-ethylenediamideanthracene-9,10-dione TFA salt as a yellow solid (0.0019 mol, 97%).

^{1}H NMR (DMSO-d_6): δ 9.13 (t, J = 5.3 Hz, 2 H), 8.69 (d, J = 1.5 Hz, 2H), 8.38 (dd, J = 8.2 and 1.5 Hz, 2H), 8.33 (d, J = 8.2 Hz, 2H), 8.02 (bs, 6H), 3.62-3.55 (m, 4H), 3.13–3.01 (m, 4H); ^{13}C NMR (DMSO-d_6): δ **4** 181.78, 165.26, 139.02, 134.72, 133.07, 133.03, 127.09 125.68, 38.41, 37.30.

^{13}C NMR (DMSO-d_6): δ **4′** 183.45, 183.39, 166.94, 140.65, 136.43, 134.72, 134.68, 128.70, 127.32, 40.05, 38.92.

HRMS, *m*/*z*: **4** 191.0853, **4′** 191.0905, ($C_{20}H_{20}N_4O_4$ M + 2H requires 191.0815).

6.6. 2,6- or 2,7-bis-[N-(3-Fmoc-amino)-propionamide]anthracene-9,10-dione – General procedure (2,6-Fmoc-β-Ala-AQ (9 or 9′)

Commercial 2,6-diamino-anthraquinone (0.40 g, 1.68 mmol) was suspended in dry THF (60 mL) and Fmoc-β-Ala-Cl (1.36 g, 4.12 mmol) was added. The mixture was heated to reflux for 7 h and a colour change from dark red to orange was observed. The product was collected by centrifugation from the cooled solution and washed with 1 M HCl (3 × 30 mL) and acetone (3 × 30 mL). Product **9** (**9′**) was obtained as a red orange powder (1.32 g, 95%).

^{1}H NMR (DMSO-d_6): δ 10.59 (s, 2H), 8.50 (d, J = 1.8 Hz, 2H), 8.15 (d, J = 8.3 Hz, 2H), 8.06 (dd, J = 8.3 and 1.8 Hz, 2H), 7.86 (dd, J = 7.4 and 0.9 Hz, 4H), 7.68 (dd, J = 7.4 and 0.9 Hz, 4H), 7.46 (t, J = 5.4 Hz, 2H), 7.38 (dt, J = 7.4 and 0.9 Hz, 4H), 7.29 (dt, J = 7.4 and 0.9 Hz, 4H), 4.27 (d, J = 6.4 Hz, 4H), 4.21 (t, J = 6.5 Hz, 2H), 3.33 (t, J = 6.3 Hz, 4H), 2.59 (t, J = 6.3 Hz, 4H).

6.7. 2,6- or 2,7-bis-(3-amino-propionamide)-anthracene-9,10-dione di-trifluoroacetate—General procedure (2,6-β-Ala-AQ TFA) (10 or 10′)

6.7.1. First step. 2,6-Fmoc-β-Ala-AQ **9** (0.84 g, 1.00 mmol) was dissolved in DMF (54 mL) and piperidine (6 mL). The solution was stirred 2 h at room temperature and then poured in Et_2O (250 mL). The free base was collected by centrifugation of the resulting suspension, washed with Et_2O (3 × 50 mL) then with water (3 × 50 mL) and dried.

6.7.2. Second step. The free base was dissolved in TFA/water 9/1 (20 mL), stirred 2 h at rt and then poured in Et_2O (150 mL). The product was collected by centrifugation, washed with Et_2O (3 × 50 mL) then water (3 × 50 mL) and dried. **10** was obtained as red/orange solid (0.56 g, overall yield 92%).

^{1}H NMR (DMSO-d_6): δ 10.76 (s, 2H), 8.53 (d, J = 1.8 Hz, 2H), 8.18 (d, J = 8.3 Hz, 2H), 8.01 (dd, J = 8.3 and 1.8 Hz, 2H), 7.75 (bs, 6H), 3.12 (m, 4H), 2.77 (t, J = 6.5 Hz, 4H). ^{13}C NMR (DMSO-d_6): δ 181.6, 169.7, 144.6, 134.6, 128.8, 128.4, 123.8, 116.2, 34.95, 33.75. HRMS, *m*/*z*: 191.0865, ($C_{20}H_{20}N_4O_4$ M + 2H requires 191.0815).

6.7.3. Taq polymerase assay. Compounds were assayed against Taq polymerase using pBR322 (2.5 ng) as a DNA template and appropriate primer sequences (0.5 μM) to amplify the 906–1064 sequence of plasmid by PCR. The reaction was carried out in a Perkin-Elmer thermocycler performing 25 cycles of: 30 s at 94 °C, 30 s at 65 °C and 30 s at 72 °C. The reaction products were resolved on a 2% agarose gel in TBE 1X (89 mM TRIS base, 89 mM boric acid, 2 mM Na_2EDTA) and stained with ethidium bromide.

6.7.4. Telomerase activity assay. An aliquot of 5×10^6 JR8 cells in exponential phase of growth was pelleted and lysed for 30 min on ice using 100 μl of 0.5% CHAPS, 1 mM EGTA, 25% 2-mercaptoethanol, 1.74% PMSF and 10% w/v glycerol. The lysate was centrifuged at 13000 rpm for 30 min at 4 °C and the supernatant collected, stored at −80 °C, and used as the telomerase source.

Telomerase activity was assayed using a modified telomere repeat amplification protocol (TRAP) assay.[8] Briefly, a proper primer (TS) was 5′-labeled with [γ-^{32}P]ATP and T4 polynucleotide kinase. After enzyme inactivation (85 °C for 5 min), a 50 μl TRAP reaction mix (50 μMdNTPs, 0.2 μg labelled TS, 0.1 μg return primer ACX, 500 ng proteic extract, 2 U *Taq* polymerase) was prepared in the presence/absence of increasing drug concentration. An internal control template (0.01 mol TSNT) with its return primer (1 ng NT) was added to the reaction mixture. Then, telomerase elongation step was performed (30 min at 30 °C) followed by a PCR amplification step (30 cycles of: 30 s at 37 °C and 30 s at 58 °C). The reaction products were loaded onto a 10% polyacrylamide gel (19:1) in TBE. Gels were transferred to Whatman 3MM paper, dried under vacuum at 80 °C and read using a phosphorimager apparatus (Amersham).

Values were expressed as percent of telomerase inhibition relative to control (no drug) lanes.

6.7.5. Fluorescence melting studies. Fluorescence melting experiments were performed in a Roche Light Cycler, using excitation at 488 nm and recording fluorescence emission at 520 nm. Oligonucleotides labelled with fluorescein (FAM) at the 5′-end of the oligonucleotide and Methyl Red (MeRed) at 3′-end were synthesized and HPLC purified by OSWEL Research Products Ltd (Southampton, UK).

Melting experiments were performed in a total volume of 20 μL containing 0.25 μM quadruplex forming labelled oligonucleotide and variable concentrations of test derivatives in LiP buffer (10 mM LiOH; 50 mM KCl pH 7.4 with H_3PO_4). Alternatively, the quadruplex-forming sequence was annealed with its complementary sequence and then submitted to the melting

procedure in the presence/absence of added drugs under the above conditions.

Mixtures were denatured by heating to 95 °C at a rate of 0.1 °C min^{-1} and T_m values were determined from the first derivatives of the melting profiles using the Roche LightCycler software.

6.7.6. Computational methods for analyzing conformers. All computational modeling studies were carried out on a 10 AMD64-CPU linux cluster running under openMosix architecture.

All described compounds were built using the 'Builder' module of Molecular Operation Environment (MOE, version 2005.06). They were minimized using the MMFF94 atom force field,[13] implemented in the MOE modeling package, until the *rms* value using the Truncated Newton method (TN) was <0.001 kcal mol^{-1} $Å^{-1}$. Partial charges have been calculated using the point electrostatic potential (ESP) charge approach implemented in the MOPAC (v.7) program as part of the MOE suite. To model the effects of solvent more directly, a set of electrostatic interaction corrections were used. MOE suite implemented a modified version of GB/SA contact function described by Still and co-authors.[14] Conformational analyses were performed using the 'Dihedral Energy Plot' module implemented in the MOE suite.

Acknowledgments

This work was carried out with the financial support from the University of Padova, Italy, the Italian Ministry for University and Research (MIUR), Rome, Italy, EU (Grant HPRN-CT-2000-00009) and Cancer Research UK. The scientific and technical partnership of Chemical Computing Group is gratefully acknowledged (Padua).

References and notes

1. Greider, C. W. *Cell* **2001**, *97*, 419.
2. Blackburn, E. H. *Cell* **2001**, *106*, 61.
3. (a) Greider, C. W.; Blackburn, E. H. *Cell* **1987**, *51*, 887; (b) Autexier, C.; Lue, N. F. *Ann. Rev. Biochem.* **2006**, *75*, 493.
4. (a) Kim, N. W.; Piatyszek, M. A.; Prowse, K. R.; Harley, C. B.; West, M. D.; Ho, P. L. C.; Coviello, G. M.; Wright, W. E.; Weinrich, R.; Shay, J. W. *Science* **1994**, *266*, 2011; (b) Counter, C. M.; Hirte, H. W.; Bacchetti, S.; Harley, C. M. *Proc. Natl. Acad. Sci. U.S.A.* **1994**, *91*, 2900; (c) Shay, J. W.; Bacchetti, S. *Eur. J. Cancer* **1997**, *33*, 787.
5. (a) Oganesian, L.; Bryan, T. M. *Bioessays* **2007**, *29*, 155; (b) Shay, J. W.; Wright, W. E. *Nature Rev. Drug Discov.* **2006**, *5*, 577; (c) Neidle, S.; Parkinson, G. N. *Nature Rev. Drug Discov* **2002**, *1*, 383; (d) Kelland, L. R. *Eur. J. Cancer* **2005**, *41*, 971.
6. See for example: (a) Sun, D.; Thompson, B.; Cathers, B. E.; Salazar, M.; Kerwin, S. M.; Trent, J. O.; Jenkins, T. C.; Neidle, S.; Hurley, L. H. *J. Med. Chem.* **1997**, *40*, 2113; (b) Kim, M. Y.; Vankayalapati, H.; Shin-Ya, K.; Wierzba, K.; Hurley, L. H. *J. Amer. Chem. Soc.* **2002**, *124*, 2098; (c) Leonetti, C.; Amodei, S.; D'Angelo, C.; Rizzo, A.; Benassi, B.; Antonelli, A.; Elli, R.; Stevens, M. F. G.; D'Incalci, M.; Zupi, G.; Biroccio, A. *Mol. Pharmacol.* **2004**, *66*, 1138; (d) Moore, M. J.; Schultes, C. M.; Cuesta, J.; Cuenca, F.; Gunaratnam, M.; Tanious, F. A.; Wilson, W. D.; Neidle, S. *J. Med. Chem* **2006**, *49*, 582; (e) Barbieri, C. M.; Srinivasan, A. R.; Rzuczek, S. G.; Rice, J. E.; LaVoie, E. J.; Pilch, D. S. *Nucleic Acids Res.* **2007**, *35*, 3272.
7. (a) Incles, C. M.; Schultes, C. M.; Kempski, H.; Koehler, H.; Kelland, L. R.; Neidle, S. *Mol. Cancer Ther.* **2004**, *3*, 1201; (b) Pennarun, G.; Granotier, C.; Gauthier, L. R.; Gomez, D.; Hoffschir, F.; Mandine, E.; Riou, J.-F.; Mergny, J.-L.; Mailliet, P.; Boussin, F. D. *Oncogene* **2005**, *24*, 2917; (c) Gomez, D.; O'Donohue, M.-F.; Wenner, T.; Douarre, C.; Macadré, J.; Koebel, P.; Giraud-Panis, M.-J.; Kaplan, H.; Kolkes, A.; Shin-ya, K.; Riou, J.-F. *Cancer Res.* **2006**, *66*, 6908; (d) Gunaratnam, M.; Greciano, O.; Martins, C.; Reszka, A. P.; Schultes, C. M.; Macadré, J.; Riou, J.-F.; Neidle, S. *Biochem. Pharmacol.* **2007**, *74*, 679.
8. (a) Collier, D. A.; Neidle, S. J. *Med. Chem.* **1988**, *31*, 874; (b) Lown, J. W.; Morgan, A. R.; Yen, S. F.; Wang, Y. H.; Wilson, W. D. *Biochemistry* **1985**, *24*, 4028; (c) Perry, P. J.; Gowan, S. M.; Reszka, A. P.; Polucci, P.; Jenkins, T. C.; Kelland, L. R.; Neidle, S. *J. Med. Chem.* **1998**, *41*, 3253; (d) Perry, P. J.; Reszka, A. P.; Wood, A. A.; Read, M. A.; Gowan, S. M.; Dosanjh, H. S.; Trent, J. O.; Jenkins, T. C.; Kelland, L. R.; Neidle, S. *J. Med. Chem.* **1998**, *41*, 4873; (e) Agbandje, M.; Jenkins, T. C.; McKenna, R.; Reszka, A. P.; Neidle, S. *J. Med. Chem.* **1992**, *35*, 1418.
9. Kim, N. W.; Piatyszek, M. A.; Prowse, K. R.; Harley, C. B.; West, M. D.; Ho, P. L.; Coviello, G. M.; Wright, W. E.; Weinrich, S. L.; Shay, J. W. *Science* **1994**, *266*, 2011.
10. Sissi, C.; Lucatello, L.; Krapcho, A. P.; Maloney, D. J.; Boxer, M. B.; Camarasa, M. V.; Pezzoni, G.; Menta, E.; Palumbo, M. *Bioorg. Med. Chem.* **2007**, *15*, 555.
11. (a) Risitano, A.; Fox, K. R. *Biochemistry* **2003**, *42*, 6507; (b) Darby, R. A. J.; Sollogoub, M.; McKeen, C.; Brown, L.; Risitano, A.; Brown, M.; Brown, T.; Fox, K. R. *Nucleic Acids Res.* **2002**, *30*, e39; (c) De Cian, A.; Guittat, L.; Kaiser, M.; Saccà, B.; Amrane, S.; Bourdoncle, A.; Alberti, P.; Teulade-Fichou, M.-P.; Lacroix, L.; Mergny, J.-L. *Methods* **2007**, *42*, 183.
12. (a) Staab, H. A.; Sauer, M. *Liebigs Ann. Chem.* **1984**, 742; (b) Broene, R. D.; Diedirich, F. *Tetrahedron Lett.* **1991**, *32*, 5227.
13. Halgren, T. *J. Comput. Chem.* **1996**, *17*, 490.
14. Qiu, D.; Shenkin, S.; Hollinger, F. P.; Still, W. C. *J. Phys. Chem.* **1997**, *101*, 3005.
15. Parkinson, G. N.; Lee, M. P.; Neidle, S. *Nature* **2002**, *417*, 87.